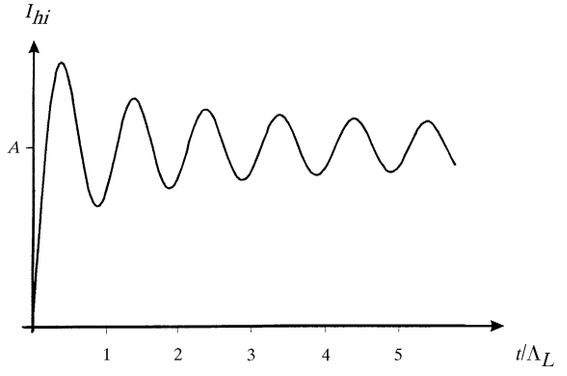

Fig. 5.1.6.7. Variations with crystal thickness of the integrated intensity in the transmission case (no absorption) (arbitrary units). The expression for A is given in the text.

$$A = \frac{R\lambda^2|CF_h|(\gamma)^{1/2}}{2V\sin 2\theta}.$$

Fig. 5.1.6.7 shows the variations of the integrated intensity with t/Λ_L.

5.1.6.5.2. *Absorbing crystals*

The integration was performed for absorbing crystals by Kato (1955). The integrated intensity in this case is given by

$$I_{hi} = A|F_h/F_{\bar{h}}|\exp\left[-1/2\mu_o t(\gamma_o^{-1}+\gamma_h^{-1})\right] \times \left[\int_0^{2\pi t\Lambda_L^{-1}} J_0(z)\,\mathrm{d}z - 1 + I_0(\zeta)\right],$$

where

$$\zeta = \mu_o t\left\{\left[|C|^2|F_{ih}/F_{io}|^2\cos^2\varphi + (\gamma_h-\gamma_o)/(4\gamma_o\gamma_h)\right]/(\gamma_o\gamma_h)\right\}^{1/2}$$

and $I_0(\zeta)$ is a modified Bessel function of zeroth order.

5.1.6.6. *Thin crystals – comparison with geometrical theory*

Using (5.1.6.6) and (5.1.6.7), the reflecting power of the reflected beam may also be written

$$I_h = \pi^2 t^2 \Lambda_o^{-2} f(\eta),$$

where

$$f(\eta) = \left[\frac{\sin U(1+\eta^2)^{1/2}}{U(1+\eta^2)^{1/2}}\right]^2$$

and

$$U = \pi t \Lambda_o^{-1}.$$

When $t\Lambda_o^{-1}$ is very small, $f(\eta)$ tends asymptotically towards the function

$$f_1(\eta) = \left[\frac{\sin U\eta}{U\eta}\right]^2$$

and I_h towards the value given by geometrical theory. The condition for geometrical theory to apply is, therefore, that the crystal thickness be much smaller than the *Pendellösung* distance. In practice, the two theories agree to within a few per cent for a crystal thickness smaller than or equal to a third of the *Pendellösung* distance [see Authier & Malgrange (1998)].

5.1.7. Intensity of plane waves in reflection geometry

5.1.7.1. *Thick crystals*

5.1.7.1.1. *Non-absorbing crystals*

Rocking curve. The geometrical construction in Fig. 5.1.3.5 shows that, in the Bragg case, the normal to the crystal surface drawn from the extremity of the incident wavevector intersects the dispersion surface either at two points of the same branch, P_1, P_1', for branch 1, P_2, P_2' for branch 2, or at imaginary points. It was shown in Section 5.1.2.6 that the propagation of the wavefields inside the crystal is along the normal to the dispersion surface at the corresponding tie points. Fig. 5.1.3.5 shows that this direction is oriented towards the outside of the crystal for tie points P_1' and P_2'. In a very thick crystal, these wavefields cannot exist because there is always a small amount of absorption. One concludes that in the thick-crystal case and in reflection geometry, only one wavefield is excited inside the crystal. It corresponds to branch 1 on the low-angle side of the rocking curve and to branch 2 on the high-angle side. Using the same approximations as in Section 5.1.6.2, the amplitude $\mathbf{D}_\mathbf{h}^{(a)}$ of the wave reflected at the crystal surface is obtained by applying the boundary conditions, which are particularly simple in this case:

$$\mathbf{D_o} = \mathbf{D_o}^{(a)},\ \mathbf{D_h}^{(a)} = \mathbf{D_h}.$$

The reflecting power is given by an expression similar to (5.1.6.7):

$$I_h = |\gamma||\xi_j|^2,$$

where the expression for ξ_j is given by (5.1.3.12), and $j = 1$ or 2 depending on which wavefield propagates towards the inside of the crystal. When the normal to the entrance surface intersects the dispersion surface at imaginary points, *i.e.* when $-1 < \eta < +1$,

$$|\xi|^2 = |\gamma|^{-1},\ I_h = 1, \qquad (5.1.7.1)$$

and there is *total reflection.* Outside the total-reflection domain, the reflecting power is given by

$$I_h = \left[|\eta| - (\eta^2-1)^{1/2}\right]^2. \qquad (5.1.7.2)$$

The rocking curve has the well known top-hat shape (Fig. 5.1.7.1). Far from the total-reflection domain, the curve can be

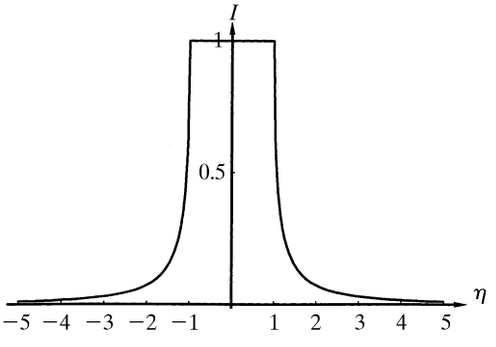

Fig. 5.1.7.1. Theoretical rocking curve in the reflection case for a non-absorbing thick crystal in terms of the deviation parameter.

references